HHS Public Access

Author manuscript

Biochim Biophys Acta. Author manuscript; available in PMC 2017 January 01.

Published in final edited form as:

Biochim Biophys Acta. 2016 January ; 1860(1 0 0): 304–314. doi:10.1016/j.bbagen.2015.06.014.

Differences in solution dynamics between lens β-crystallin homodimers and heterodimers probed by hydrogen–deuterium exchange and deamidation

Kirsten J. Lampi[a,*], **Matthew R. Murray**[a], **Matthew P. Peterson**[a], **Bryce S. Eng**[a], **Eileen Yue**[b], **Alice R. Clark**[c], **Elisar Barbar**[d], and **Larry L. David**[b]

Kirsten J. Lampi: lampik@ohsu.edu

[a]Integrative Biosciences, Oregon Health & Science University, Portland, OR 97239-3098, United States

[b]Biochemistry and Molecular Biology, Oregon Health & Science University, Portland, OR 97239-3098, United States

[c]Birkbeck College, University of London, United Kingdom

[d]Biochemistry and Biophysics, Oregon State University, Corvallis, OR 97331, United States

Abstract

Background—Lens transparency is due to the ordered arrangement of the major structural proteins, called crystallins. βB2 crystallin in the lens of the eye readily forms dimers with other β-crystallin subunits, but the resulting heterodimer structures are not known and were investigated in this study.

Methods—Structures of βA3 and βB2 crystallin homodimers and the βA3/βB2 crystallin heterodimers were probed by measuring changes in solvent accessibility using hydrogen–deuterium exchange with mass spectrometry. We further mimicked deamidation in βB2 and probed the effect on the βA3/βB2 heterodimer. Results were confirmed with chemical crosslinking and NMR.

Results—Both βA3 and βB2 had significantly decreased deuterium levels in the heterodimer compared to their respective homodimers, suggesting that they had less solvent accessibility and were more compact in the heterodimer. The compact structure of βB2 was supported by the identification of chemical crosslinks between lysines in βB2 within the heterodimer that were inconsistent with βB2's extended homodimeric structure. The compact structure of βA3 was supported by an overall decrease in mobility of βA3 in the heterodimer detected by NMR.

In βB2, peptides 70–84 and 121–134 were exposed in the homodimer, but buried in the heterodimer with ≥50% decreases in deuterium levels. Homologous peptides in βA3, 97–109 and 134–149, had 25–50% decreases in deuterium levels in the heterodimer. These peptides are probable sites of interaction between βB2 and βA3 and are located at the predicted interface

[*]Corresponding author at: Integrative Biosciences, Oregon Health & Science University, Room RJH 7337, 3181 SW Sam Jackson Park Road, #L595, Portland, OR 97239-3098, United States.

Supplementary data to this article can be found online at http://dx.doi.org/10.1016/j.bbagen.2015.06.014.

between subunits with bent linkers. Deamidation at Q184 in βB2 at this predicted interface led to a less compact βB2 in the heterodimer.

The more compact structure of the βA3/βB2 heterodimer was also more heat stable than either of the homodimers.

Conclusions—The major structural proteins in the lens, the β-crystallins, are not static, but dynamic in solution, with differences in accessibility between the homo-and heterodimers. This structural flexibility, particularly of βB2, may facilitate formation of different size higher-ordered structures found in the transparent lens.

General significance—Understanding complex hetero-oligomer interactions between β-crystallins in normal lens and how these interactions change during aging is fundamental to understanding the cause of cataracts.

Keywords

β-Crystallins; Deamidation; Lens; Cataracts; Solution dynamics; Hydrogen; deuterium exchange; Mass spectrometry

1. Introduction

The lens is unique from other organs in that it is optically transparent. This is in order for the lens to focus light onto the retina. Lens transparency is due to the short-range ordered arrangement of the major structural proteins, the α, β and γ-crystallins that are present in the cytosol at 300–500 mg/ml [1]. At these high concentrations, short-range interactions between nearby atoms contribute to the compact structures of the crystallins and to their close packing giving the lens a dense liquid or glass-like structure [2,3]. The dynamic polydispersity of the oligomeric α-crystallins and possibly the β-crystallins prevents crystallization or precipitation of the soluble crystallins in the normal lens [4,5].

The two-domain compact structures of the related monomeric γ-crystallins and oligomeric β-crystallins have been well characterized, with several structures solved from the members of the β/γ-crystallin family [6-10]. There are extended or compact main structures for the β-crystallin monomers depending on the conformation of the connecting peptide (extended or bent, respectively) between the two domains within each crystallin subunit.

In βB2, which has an extended structure, the N- and C-terminal domains are joined together by an extended connecting peptide [6]. In the homodimer, this allows swapping of the domains between subunits where the N-terminal domain of one subunit interacts with the C-terminal domain of the partner subunit. This interdomain interaction is across a pseudo 2-fold axis of symmetry called the P dyad (PQ interface) in the crystal structure. This PQ interface is stabilized by hydrophobic interactions and salt bridges and has been shown by our laboratory to be extremely solvent inaccessible by hydrogen-deuterium exchange (HDX) [11].

In contrast to βB2, the connecting peptide in βB1 is bent allowing the N- and C-domains to be paired intrachain, giving the dimer a compact structure with both inter- and intradomain interfaces. The intradomain interface in βB1 is equivalent to the interdomain (PQ) interface

in βB2. The additional interface between the domains of the partner βB1 subunits is the RQ interface in the crystal structure [7]. Both interfaces are stabilized by hydrophobic interactions and salt bridges and contribute to βB1's more compact structure and greater thermodynamic stability compared to βB2 [12–14]. More recently, the crystal structures of βA4 and βB3 have also been solved (PDB:3LWK and 3QK3, respectively, Structural Genomics Consortium, 2010) and predict compact structures like βB1 with bent linkers that result in two interfaces within the homodimers. The structure of βA3 is not known, but it has been predicted to undergo a concentration-dependent equilibrium between extended and bent conformations [15,16].

Despite what we know about the homodimers, the lack of structural information about the hetero-oligomers–which are found in vivo–remains a major obstacle to understanding lens transparency. Stable hetero-oligomers readily form between the basic and acidic β-crystallin subunits [12,16-20]. βB1 and βA3 preferentially form a tetramer, while βB2 and βA3 preferentially form a heterodimer [18,19]. Changes in the conformation of the polypeptide chains have been observed by changes in the spectroscopic properties of the proteins, but the exact nature of the conformational changes have not been described. The βA3/A1, βB1, and βB2 crystallins are the most abundant β-crystallins in the human lens, with βB1 and βA3 the most modified during aging and cataracts [21,22]. The simpler βA3/βB2 heterodimer was chosen to investigate in this study by HDX, with future experiments planned to investigate the more complex tetramer.

Our laboratory has previously determined the solution dynamics of the βB2 homodimer by probing the solvent accessibility using HDX measured by mass spectrometry [11]. Regions with low deuterium incorporation are inaccessible to the solvent, suggesting either buried locations or surface regions involved in protein-protein interactions. Using these methods, we have observed that the monomer-monomer interface region in βB2 is particularly solvent inaccessible [11], less than 15% deuterium was exchanged, suggesting a “tight” interaction and a slow rate of subunit exchange between stable dimers.

During both aging and cataracts, crystallins accumulate many modifications that are associated with an increase in insoluble proteins isolated from donor lenses [22]. These modifications are expected to disrupt normal interactions between crystallins. We have identified deamidation of Asn and Gln residues as a major age-related modification in lens [21,22]. By mimicking deamidation in vitro, we have determined that deamidation increases solvent accessibility between interacting monomers in βB2, providing a mechanism for the deamidation-induced decreases in its stability [11,14]. In this study, we characterize the βA3/βB2 heterodimer using HDX and mimicked deamidation in βB2 to probe its effect on interface interactions in the heterodimer structure.

2. Methods and materials

2.1. Protein expression and purification

The recombinant expression and purification of untagged wild type (WT) βA3, WT βB2 crystallin, and the deamidated mimics of βB2 (βB2Q70E and βB2Q184E) was carried out using *Escherichia coli* as previously described [14,23]. Confirmation of purity was

estimated by SDS-PAGE to be > 90% and mass spectrometry confirmed the predicted masses. Crystallins were then concentrated and dialyzed into buffer specific to experimentation. Protein concentrations were determined by absorbance at 280 nm using a NanoDrop UV/Vis spectrophotometer (Thermo Scientific, Waltham, MA). A theoretical Abs_{280} extinction coefficient of 2.6 $(mg/ml)^{-1}$ cm^{-1} was used for βA3, and 1.7 $(mg/ml)^{-1}$ cm^{-1} for βB2.

2.2. Formation of βA3/βB2 heterodimer

Following purification, proteins were buffer exchanged into 100 mM sodium-phosphate (pH 7.4), 1 mM EDTA, 2.5 mM TCEP, and 100 mM KCl (HDX buffer). In order to form a heterocomplex from βB2 and βA3 homodimers, both proteins were mixed together at equal molar concentrations at 37 °C for 18 h. The polydispersity of the resulting mixtures was determined by size-exclusion chromatography in-line with multi-angle laser scattering (MALS) on a DAWN HELEOS instrument (Wyatt Technology Inc., Santa Barbara, CA). Polydispersity was measured as the weight-averaged molecular weight divided by the number-averaged molecular weight measured by light scattering using ASTRA software (Wyatt Technology Inc.). This confirmed that βA3 and βB2 preferentially form heterodimers after overnight incubation as previously reported [19], and that the selected deamidations did not prevent the subunit exchange.

2.3. Hydrogen deuterium exchange of β-crystallins

In order to probe changes in solvent accessibility between homodimeric and heterodimeric structures, HDX was performed for both βB2 and βA3 crystallin homodimers and these results compared to the HDX of βA3/βB2-crystallin heterodimers. Deuterium labeling was done as previously described with the following modifications: a 12 μL sample from an overnight incubation of the crystallin oligomer containing 80 μM of each protein was diluted 10-fold by combining with 108 μL of HDX buffer, prepared with D_2O. HDX was performed at 4 °C for 0, 10, 100, 1000, and 10,000 s[24]. At each time point, the deuterated sample was combined with an equal volume of quenching buffer (0.42% phosphoric acid). These samples were then immediately flash-frozen in liquid nitrogen and stored at −70 °C for less than one week before mass spectrometry was performed.

Frozen samples were thawed and immediately analyzed using proteolytic digestion and mass spectrometry. A 40 μL quenched sample described above was added to 18 μL of 8 M urea, a 2 μL sample of saturated protease from *Aspergillus saitoi*, Type XIII (Sigma, St. Louis, MO) in 50mM sodium citrate buffer, pH3, was added, and digestion performed for 2 min in an ice bath [25]. Liquid chromatography/mass spectrometric (LC/MS) analysis was then immediately performed as previously described using an LTQ-Orbitrap Discovery Instrument (Thermo Scientific, San Jose, CA) with peptide trap/chromatography column on ice, except MS scans were collected at a resolution of 30,000 with an m/z range of 400–1500 [11]. One tandem mass spectrometry analysis of each sample was performed using identical chromatographic conditions to identify peptides by alternating survey MS scans in the Orbitrap mass analyzer with three data-dependent MS/MS scans in the linear ion trap using collision-induced dissociation, and the dynamic exclusion feature of the instrument's control software.

Peptides and their retention times were identified using Sequest software and peptide lists and retention times exported for use by either HD Desktop as previously described [24] or by HD Examiner (Sierra Analytics, Modesto, CA) with similar results. The sequences of βA3 and βB2 crystallin peptides identified following protease digestion were used to calculate their expected isotopic distributions and average masses. The sample immediately quenched at 0 s was used as the non-deuterated control to determine the shift in peptide masses following HDX at different time points. The exchange rates of peptides derived from βA3 and βB2 homodimers were each compared to their respective exchange rates in peptides derived from βA3/βB2 heterodimer. Peptide fragments identified by MS/MS analysis were manually selected based on the quality of mass spectra across samples, and average masses of exchanged peptides calculated by HD Examiner or HD Desktop. Three independent repeats were performed for each sample. The number of deuterons exchanged into each peptide at different time points was exported into either Microsoft Excel or GraphPad Prism to identify peptides with statistically different exchange rates relative to control using a t-test (Student's t-test or the Holm-Sidak method, with a = 5.000%).

2.4. NMR analysis of β-crystallins

A uniformly ^{15}N-labeled βA3-crystallin homodimer was produced from *E. coli* grown in ^{15}N medium. ^{1}H-^{15}N heteronuclear single quantum coherence (HSQC) spectra were collected both from this ^{15}N heteronuclear single quantum coherence (HSQC) labeled βA3-crystallin homodimer and from a βA3/βB2-heterodimer, but containing a ^{15}N labeled βA3 subunit. Data were collected on a 700 MHz Bruker spectrometer at 5 and 37 °C.

Disordered regions were characterized by spectra with limited dispersion in the amide region spanning 8–8.5 ppm instead of 7–11 ppm expected for folded proteins [26]. In addition, disordered segments with sharp peaks were distinguished from the extensively broad peaks arising from the large ordered domains. Large folded proteins have long correlation time due to slow tumbling but disordered segments within the same protein tumble at much higher rate [27].

2.5. Crosslinking of heterodimers

WT βA3 and βB2 crystallin homodimers or βA3/βB2 mixtures were incubated overnight at 37 °C, dialyzed into 20 mM sodium phosphate, 150 mM NaCl (pH 7) and subjected to chemical crosslinking using an equalmolar mixture of undeuterated and deuterated forms of CyanurBiotinDimercaptoProprionylSuccinimide (CBDPS) crosslinker with a 14 Å span (Creative Molecules, Inc. Vancouver, CAN). CBDPS was dissolved immediately before use in anhydrous DMSO at a 1.25 mM concentration and diluted 10 fold into the crystallin solutions that were at approximately 1 mg/ml concentration. Following incubation at room temperature for 30 min, the reaction was quenched by addition of an equal volume of 100 mM ammonium bicarbonate and samples dried by vacuum centrifugation. The samples were then dissolved in 8 M urea, reduced, alkylated, urea diluted to 2 M concentration, and digested overnight with trypsin as previously described [28]. Peptides reacting with CBDPS were purified using cation exchange and avidin affinity chromatography (ICAT labeling kit, AB SCIEX, Redwood City, CA). Purified peptides were then separated using a Dionex NCS-3500RS UltiMate RSLCnano UPLC system and PepMap RSLC C18, 2 μm, 75 μm ×

50 cm EasySpray column (Thermo Scientific), 2–30% ACN gradient over 100 min at a 300 nl/min flow rate in a mobile phase containing 0.1% formic acid. Mass spectrometric analysis used an EasySpray nanosource and Orbitrap Fusion Tribrid mass spectrometer (Thermo Scientific). Survey scans from m/z = 350–1600 at 120,000 resolution and MS/MS scans at 60,000 resolution were both collected in the Orbitrap mass analyzer, using a 1.6 Da quadrupole isolation, collision-induced dissociation in the ion trap, 40 s dynamic exclusion time with a repeat count of 1, charge state selection between 3–7, monoisotopic precursor selection filter on, detection properties set to top speed, and a 5-s dwell time between survey scans. The user defined lock mass feature was also used by monitoring a m/z = 445.12 polysiloxane ion. Results were analyzed using StavroX software (v3.4.9) [29]. A maximum mass deviation of 10 ppm for precursor and 20 ppm for fragment ions between theoretical and experimental mass was allowed. Searches used a database consisting of βA3 and βB2 crystallin sequences, required score values in excess of matches to sequence reversed peptides, and were manually inspected to assess assignment of fragment ions to both crosslinked peptides.

2.6. Heat stability of heterodimers

βA3 and βB2 homodimers and βA3/βB2 heterodimers were produced as described above and heated to 55 °C. The turbidity of each solution was measured as the change in optical density at 405 nm and the percent of the maximum OD was reported [30].

3. Results

3.1. Formation of βA3/βB2 heterodimer

Our goal was to characterize the heterodimer of βA3/βB2 to shed light on the complex protein–protein interactions that determine transparency in the lens. Following the bacterial expression of βA3 and βB2 crystallins, the last step of their purification used size-exclusion chromatography with in-line determination of molar masses by light scattering. We have previously reported that the homodimers eluted with symmetrical peaks and molar masses of 49 ± 2 and 45 ± 3 kDa for βA3 and βB2, respectively [14,23]. The theoretical molecular weights are 50.3 kDa for βA3 and 46.5 kDa for βB2. After 90 min at 37 °C, the βA3/βB2-heterodimer eluted in a nonsymmetrical peak with a sharp leading edge of 64 kDa and a sloped tailing edge of 45 kDa [31]. Results were repeated in this study. Immediately upon mixing, βA3- and βB2-crystallins eluted in a broad peak with a polydispersity of 1.03. After 18 h at 37 °C, the βA3/βB2-heterodimer eluted in a symmetrical peak with a polydispersity index of 1.00 (Fig. 1A). The weight-average molecular weight of this peak is 51.1 kDa. The distribution of the species was 90% between 49–52 kDa.

These βA3 and βB2 crystallin homodimers were analyzed using BN:PAGE (Fig. 1B, lanes 1 and 2). The incubated βA3 homodimer (lane 3, arrow a), βB2 homodimer (lane 4, arrow b), and βA3/βB2 heterodimer (lane 5, arrow c) each migrated on BN:PAGE with a major band distinct from each other. This result confirmed the previous finding that βA3 and βB2 homodimers spontaneously undergo subunit exchange when mixed to form a heterodimer [19].

Based on migration distances, BN:PAGE indicated that βA3 had the most compact structure, βB2 the least compact, and that βA3/βB2 heterodimer adopted a structure of intermediate size, migrating to a position close to βA3 homodimer.

3.2. Changes in solvent accessibility between βB2 and βA3 homodimers and heterodimer

The different migration patterns on BN:PAGE suggested that βB2 and βA3 had conformations in the heterodimer (Fig. 1, lane 5) that were different from their homodimer conformations (lanes 3 and 4). To test this, we compared the HDX rates between homodimers and heterodimers for βA3 and βB2. Exchange times that ranged from 10 to 10,000 s were used so that we could compare differences in both fast and slow exchanging residues. These data are shown in Supplemental Figs. 1 and 2, and demonstrated that for most regions of the protein, the greatest differences were observed after 1000 s of exchange.

The results following 1000 s of exchange for βB2 are shown in Fig. 2, where the extent of deuterium incorporation in peptides in the homodimer (black bars) and heterodimer (white bars) are compared. The βB2 regions analyzed were restricted to peptides that were identified in digests of both homodimers and heterodimers. We will use residue numbers starting from the actual protein N-terminus (initial methionine lost), which differs from residue numbers in UniProt (www.uniport.org). We found the greatest deuterium incorporation (>25%) in the βB2 homodimer in peptides from the N- and C-terminal extensions, peptide 4–21, peptide 191–204, as well as in peptides at exposed loops (peptide 34–52 and peptide 126–139). Additional peptides with high exchange were peptide 70–84 and peptide 170–184, located on the exposed RQ surface; and peptide 95–102, containing part of the connecting peptide between the N-terminal domain (N-td) and C-terminal domain (C-td) [8]. The RQ surface is at the interface between two βB2 homodimers when they form a tetramer, but remains exposed in the βB2 homodimer (Fig. 3).

We found the lowest deuterium incorporation (<10%) in the C-td peptide 151–163, which is located at the predicted PQ interface between the N-td and C-td in the βB2 homodimer (Fig. 3, blue regions). We also found low incorporation in peptide 103–110, which contains the first β-strand of the third Greek Key in the C-td. Peptides with deuterium uptake between 10–25% are highlighted in yellow in Fig. 3.

The HDX results were compared to analysis of the βB2 homodimer structure in the Protein Data Base (PDB:1YTQ) using the Protein Interfaces, Surfaces, and Assemblies server (PDBePISA, http://www.ebi.ac.uk/msd-srv/prot_int/pistart.html) and were found to be in good agreement. Three peptides, 34–52, 70–84, and 126–134 (labeled in Fig. 3), had high deuterium exchange, and contained highly solvent-accessible residues. Residues within peptide 34–52 were all exposed with P36, K41, E42, and K47 having accessible surface areas equal to or greater than 100 A^2. The 70–84 peptide included the exposed residues, 76–83, with E77 and R80 having accessible surface areas greater than 100 A^2. Residues within peptide 126–134 were exposed and included two of the three adjacent Asp residues, D125, D126 and D127. Residue D126 has a calculated surface area of 94.5 A^2. Therefore, these three peptides contained residues with large calculated solvent accessibilities that also agreed with our previous HDX experimental results [11].

Since the structure of βA3 is unknown, the crystallographic structure of βA4 homodimer (PDB:3LWK) was used to predict the locations of peptides in βA3. βA3 and βA4 share 68% sequence homology overall and 75% homology in the C-td alone. We again use residue numbers starting from the actual protein N-terminus (initial methionine lost). Deuterium incorporation in the βA3 homodimer (Fig. 4) reached 50% at the flexible N-td extension in residues 1–36 (red in Fig. 5). Other regions with high levels of deuterium included the predicted connecting peptide and loop regions (peptides 48–67, 97–109, 113–123, and 140–162 in Fig. 4 and highlighted in red in Fig. 5). Within the peptide 97–109, several homologous residues (102–106) were not resolved in the βA4 crystal structure suggesting they were highly flexible. This supports the high level of deuterium incorporation that we found in this peptide. Adjacent to this flexible region in the structure are three peptides containing residues 68–96 with less than 10% deuterium incorporation (Fig. 4). These residues are located at the PQ interface between N-td and C-td regions in βA4 homodimer and extend into the RQ interface between the partner subunit (Fig. 5, blue regions). This region in βA3 homodimer had lower rates of deuterium incorporation compared to the homologous regions in βB2 homodimer, suggesting that this region was less solvent accessible in βA3 homodimer (βA3 (89-96) compared to βB2 (70-84) in Fig. 6). Additional deuterium incorporation below 10% was also observed in residues 163–183 (Fig. 5, blue regions). These results provide the first structural information for βA3 homodimer in solution and support a homodimer similar to βA4 with a bent linker between the domains (compact structure) [15].

3.3. Decreased solvent accessibility of βB2 upon incorporation into the βA3/βB2 heterodimer

The faster migration of βB2 observed by BN:PAGE (Fig. 1) when it was in complex with βA3 suggested a more compact structure that would be less solvent-accessible than when in its homodimeric form. This was confirmed by the 50–80% decrease in deuterium incorporation in βB2 peptides 53–63, 70–84, 121–125, 126–134, and 151–163 in the βB2/βA3 heterodimer (Fig. 2). Data for all time points for peptides 70–84 and 126–134 are shown in Fig. 6A and B respectively. These peptides are solvent exposed in the crystallographic structure of βB2 homodimer described above (PDB:1YTQ, Fig. 3). The decrease in deuterium incorporation in these peptides suggests that βB2 underwent a structural change, with these residues becoming less solvent accessible in the βA3/βB2 heterodimer.

To determine if the above results are expected if βB2 adopts a compact structure in the βA3/βB2 heterodimer, we compared peptides 70–84 and 126–134 to homologous regions of the βB1 homodimer structure (PDB:1OKI PDBePISA). These residues in the βB1 homodimer structure are intrachain interface residues and are highlighted in purple in Fig. 7A. While, residues 76–83 in βB2 are accessible, the homologous residues in the βB1 homodimer, 118–125, are partially inaccessible with four residues involved in hydrogen bonding with the partner subunit. Residues D126 and D127 in βB2 are also accessible with no buried surface areas, while the homologous residues in βB1, D168 and D169, have partially buried surface areas. These observations support that βB2 changes conformation in

the βA3/βB2 heterodimer and may adopt a structure similar to βB1 with a bent linker and alternate intermolecular interface.

Deuterium incorporation was not significantly altered in the N- and C-terminal extensions of βB2 (peptides 4–21 and 191–204, respectively) in the βA3/βB2 heterodimer (Fig. 2). This confirmed previous NMR results supporting that they remain unstructured in the heterodimer and thus, may not be necessary for dimer formation [32].

3.4. Decreased solvent accessibility of βA3 upon incorporation into the βA3/βB2 heterodimer

Since the NB:PAGE results in Fig. 1 suggested that the βA3 homodimer had the most compact structure, we predicted that some βA3 peptides in the βA3/βB2 heterodimer would exhibit higher rates of exchange than in the βA3-homodimer. However, βA3 peptides in the heterodimer either showed no change in deuterium incorporation or, like peptides in βB2, had decreased rates of exchange.

As in βB2, differences in βA3 exchange at 10 to 10,000 s were compared between βA3 homodimer and βA3/βB2 heterodimer (Supplemental Fig. 2). Fig. 4 summarizes the differences in exchange at 1000 s between βA3 homodimer (black bars) and βA3/βB2 heterodimer (white bars). The high deuterium incorporation in the N-td extension of βA3 (residues 1–36) in both the βA3 homodimer and βB2/βA3 heterodimer, suggest that the N-td extensions are not involved in dimer formation.

Decreased deuterium incorporation in the βA3/βB2 heterodimer was localized to the C-td with the exception of a decrease in the N-td at peptide 97–109 (Fig. 4).These peptides were mapped to the locations of homologous peptides in the βA4 structure (PDB:3LWK) and are highlighted in purple in Fig. 7B. These peptides were predicted to be at the βA4 RQ interchain interface, and in the C-td at the PQ intrachain interface. In the C-td, homologous peptides βA3 (140-149) and βB2 (126-134) were exposed in the homodimers, but buried in the heterodimer (Fig. 6B). The decreased deuterium incorporation in both βB2 and βA3 in the βA3/βB2 heterodimer and spontaneous heterodimer formation suggests increased stabilizing protein–protein interactions in heterodimers compared to homodimers.

3.5. NMR spectra confirmed less mobility of βA3 in the βB2–βA3 heterodimer than in the homodimer

NMR of heavy-labeled βA3 was performed because the structure of βA3 in solution was not known, and to confirm changes in its structure during heterodimer formation. In Fig. 8, the spectra in A show the peaks from sharper signals due to greater mobility. The only peaks in the spectra are of labeled βA3. These spectra verified that there is a region in the protein, presumably the long extensions, that were of higher mobility than the rest of the protein. The spectra were the same in the homo- and heterodimer confirming the hydrogen deuterium exchange results that the flexibility of the extensions did not change in the heterodimer.

The NMR spectra of labeled βA3 in A and B were recorded at 5°C and 35 °C, respectively. The spectra in B are plotted at a lower contour level to show the peaks that are of minor intensity and were subtracted out in A panels. The minor peaks correspond to regions of

slower tumbling and most likely to the intact protein dimer. The spectra in C were collected at 35°C to increase the tumbling rate of the protein, and thus the signal intensity. While more peaks were detected at 35 °C than at 5 °C for the homo- and heterodimers, the intensity of the minor peaks was less in the heterodimer. This difference was more apparent at 35 °C. Regions where the intensity of the minor peaks in the heterodimer (right) was lower and even disappeared are circled in red. This suggested that the intact βA3 in the heterodimer was more compact and less mobile than in the homodimer.

3.6. The effect of mutations Q70E and Q184E in βB2 on interface interactions in the βA3/βB2 heterodimer

To probe how deamidation, a major age-related modification in lens, alters heterodimeric interactions, we created βA3/βB2 heterodimers with βB2 mutants mimicking deamidations at the putative interfaces. Our laboratories have identified Gln at residues 70 and 184 in βB2 as in vivo sites of deamidation [22,33,34].

We have previously shown that Q70E mutation increases the solvent accessibility across the PQ interface in βB2 homodimer [11]. However, the Q70E mutation would not be predicted to disrupt the new RQ interface in a bent-linker model of βB2, whereas the Q184E mutation, located near the RQ interface, would be predicted to disrupt this interface [8] (see Fig. 7A). WT βA3/βB2 and heterodimers formed between WT βA3 and either βB2 Q70E or βB2 Q184E mutants were separated by BN:PAGE (Fig. 9A). Both mutants formed heterodimers that migrated just below the WT heterodimer, suggesting a slightly more compact structure.

HDX rates were determined for the βA3/βB2 heterodimers containing mutant βB2. Small, but significant, increases in solvent exposure due to the Q184E mutation, were observed for both the βB2 homodimer and βA3/βB2 heterodimer (Fig. 9B and C). However, as expected, the solvent exposure was more pronounced in the βA3/βB2 heterodimer. Deuterium incorporation in βB2 peptides 72–81 and 126–136 increased 17 and 24%, respectively, in the βA3 heterodimer with βB2 Q184E compared to 9 and 18% with βB2 WT (Fig. 9B, 1000 s). Both of these peptides are located on the RQ interface, although only peptide 126–134 would be predicted to be affected by the mutation at Q184 due to Q184's close proximity of less than 4 Å to H132 within the same polypeptide chain.

As expected, Q70E mutation in βB2 did not lead to any significant changes insolvent accessibility in βB2 within the βA3/βB2 heterodimer.

HDX rates were also determined for βA3 with in the βA3/βB2 heterodimers containing mutant βB2s (Fig. 9D). Only the mutation at Q184 affected the solvent accessibility in βA3, and instead of increasing accessibility, the accessibility was decreased. The decreased accessibility was in the long peptide 134–162 from the C-td. While, it is not clear why Q184E led to decreased accessibility, these data fit with its greater thermal stability described below.

3.7. Chemically cross-linking Lys residues in βA3/βB2 heterodimers

In order to provide further evidence of a change in conformation of βB2 in the βA3/βB2 heterodimer, experiments were performed using the chemical cross linking reagent,

CyanurBiotinDimercaptoProprionylSuccinimide (CBDPS) (Supplemental Fig. 3A). This reagent crosslinks Lys residues that are within distances of 14 Å. There are 12 Lys residues in βB2. Five of these Lys are highlighted in Fig. 10 due to their close proximity to the RQ interface. Other Lys residues that have their R groups oriented on the opposite surface of the predicted RQ interface would not be expected to form crosslinks with βA3 in the βA3/βB2 heterodimer.

Mass spectrometry identified a crosslinked peptide between K75 and K119 in βB2 within the βA3/βB2 heterodimer (supporting MS/MS spectra shown in Supplemental Fig. 3B). The location of these crosslinked residues are shown in the extended structure of the βB2 homodimer (Fig. 10). The distance between K75 and K119 is 26 Å. This distance is too great to be compatible with the extended βB2 homodimer structure. No crosslinks were identified between any of the Lys on the opposite surface of βB2 heterodimer, consistent with this surface being solvent exposed in the heterodimer. Unexpectedly, no cross-linked peptides were identified between βB2 and βA3 in the heterodimer. The lack of identified crosslinks may reflect a low number of available Lys groups at the interacting surfaces.

3.8. Differences in heat stability of βB2, βA3, βA3/βB2, βA3/B2Q70E, and βA3/βB2Q184E

In order to determine if the more compact βA3/βB2 heterodimer was also more stable than the respective homodimers, dimers were heated and the rate at which the solutions reached their maximum turbidity was measured as an indication of denaturation and precipitation. The βA3/βB2 heterodimer reached its maximum turbidity at a slower rate than did the βA3 or βB2 homodimers (Fig. 11). The βA3/βB2Q184E heterodimer reached its maximum turbidity at an even slower rate than the WT βA3/βB2 heterodimer. The βA3/βB2Q184E dimer was the most resistant dimer to heat denaturation and may reflect the more compact C-td of βA3 in the βA3/βB2Q184E heterodimer. These data are consistent with more compact dimers being more heat stable.

4. Discussion

In this study, we have examined the solution structure of a β-crystallin heterodimer and identified, for the first time, that βB2 crystallin adopts a structure quite unlike that predicted by its extended-linker structure as a homodimer. This suggested that like the resolved crystallographic structures of βB1, βB3, and βA4 homodimers, β-crystallin heterodimers might adopt a bent linker conformation containing an intramolecular PQ interface and intermolecular RQ interface. This is consistent with the conformational changes in the βB2 subunit being driven by new and favorable interactions with its heterologous partner when subunit changes occur.

We also identified potential sites of protein–protein interactions between these β-crystallin complexes. The ability of β-crystallins to take on different conformations could facilitate formation and stability of different size crystallin oligomers, potentially disrupting detrimental long-range order at the high protein concentrations found in the lens [1]. Our findings suggested that the individual crystallins are, in fact, dynamic and not just static structural proteins.

Structures of four of the seven β-crystallin subunits (crystallized as homodimers) are known. They all have homologous interfaces between the N- and C-terminal domains within the same polypeptide, or between partner subunits. Two distinct conformations have been solved: a less compact conformation (βB2) with an extended linker, and a more compact conformation with a bent linker connecting the N- and C-terminal domains (βB1, βB3, and βA4). In the domain swapped βB2 dimer, the interface is between domains from partner subunits. In the compact dimers, this same interface is between domains from the same polypeptide chain (as in all γ-crystallins) with an additional interface between the two subunits.

The crystal structures of β-crystallins heterodimers are not known. We report here for the first time that βB2 takes on a more compact and less solvent accessible structure with βA3 in the βA3/βB2 heterodimer. The domain–domain interface (equivalent to the paired domain interface in γ-crystallins) in the extended βB2 homodimer is between partner subunits. In a compact conformation of the βA3/βB2 heterodimer, this interface would now be intrachain within βB2, leaving other βB2 residues to interact with βA3. Our study identified residues in these protein–protein interaction regions from their decreased deuterium incorporation in the βA3/βB2 heterodimer. Our data were consistent with βB2 changing from an extended linker conformation in homodimers to a more βB1-like bent-linker conformation in the heterodimers with βA3. In other words, the new heterodimer interface is similar to the monomer–monomer interface of the βB1 homodimer. Our results do not preclude that the βB2 homodimer can also take on more compact dimer conformations in solution. The flexibility of βB2 in solution is an important property that would facilitate dynamic interactions with different β-subunit partners.

The structure for βA3 crystallin has not yet been solved; however, our data are in agreement with a compact βA3 structure, similar to βA4. In complex with βB2, the βA3 structure is less solvent accessible than in homodimers, most notably in the C-td. NMR spectra confirmed that βA3 was less mobile in the heterodimer than in the homodimer.

There were no changes in solvent accessibility determined in the N-td extensions of either βB2 or βA3 upon heterodimer formation, implying these extensions do not play a role in formation of the βA3/βB2-dimer. Although not determined, similar results would be expected for βA1-crystallin, which is homologous to βA3, only with an alternate start site at Met-18 in βA3. The extension of βA1 includes residues 18–30 of βA3, which were exposed in the heterodimer.

Taken together, these findings suggest that βB2 may facilitate the spontaneous formation of the heterodimer by interacting with the C-td of βA3.

Our results also highlight a potential role for flexible loop regions in the predicted buried interface interactions between βB2 and βA3. In both βB2 and βA3, two regions containing predicted (from crystal structures) surface loops were exposed in the homodimers, but less solvent accessible in the heterodimer (Figs. 3, 5, and 7). The C-td loops contain several charged residues, including three adjacent Asp residues in βB2 and two in βA3. In the heterodimer, these residues may participate in interactions similar to structures in βB1, βA4,

and βA3 homodimers with the potential for charge interactions between one of the Asp residues and a nearby Arg across the interface (PDBePISA analysis). Our HDX results suggest that these loops are sites of interaction in the βA3/βB2 heterodimer.

In conclusion, the ability of βB2 to take on different conformations depending on its partner subunit suggests that the β/γ crystallins are not just static structural proteins, but are dynamic in solution. More compact, less solvent accessible structures of β-crystallin hetero-oligomers may slow their denaturation caused by age-related modifications like deamidation. The more compact, less solvent exposed structures may also serve to slow age-related modifications. While we have shown that deamidation is capable of altering solvent accessibility in β-crystallin hetero-oligomers, crystallographic or NMR based structures of these proteins are needed to fully understand the cause of these structural perturbations that lead to crystallin aggregation and light scatter in cataract.

Supplementary Material

Refer to Web version on PubMed Central for supplementary material.

Acknowledgments

Authors wish to acknowledge grant funding sources from NIH-EY012239 (KJL), EY10572 (Core Vision grant), EY007755 (LLD) and GM084276-01 (EB) and from NSF support to Portland State University Grant 0741993. Authors wish to thank Dr. Phillip Wilmarth for the expert advice and Dr. Takumi Takata and Cade Fox for the initial experiments. This work is dedicated to the memory of Dr. Orval Bateman whose many papers provided the foundation of this current research.

References

1. Delaye M, Tardieu A. Short-range order of crystallin proteins accounts for eye lens transparency. Nature. 1983; 302:415–417. [PubMed: 6835373]
2. Veretout F, Tardieu A. The protein concentration gradient within eye lens might originate from constant osmotic pressure coupled to differential interactive properties of crystallins. Eur Biophys J. 1989; 17:61–68. [PubMed: 2766998]
3. Mirarefi AY, Boutet S, Ramakrishnan S, Kiss AJ, Cheng CH, Devries AL, Robinson IK, Zukoski CF. Small-angle X-ray scattering studies of the intact eye lens: effect of crystallin composition and concentration on microstructure. Biochim Biophys Acta. 2010; 1800:556–564. [PubMed: 20167250]
4. Laganowsky A, Benesch JL, Landau M, Ding L, Sawaya MR, Cascio D, Huang Q, Robinson CV, Horwitz J, Eisenberg D. Crystal structures of truncated alphaA and alphaB crystallins reveal structural mechanisms of polydispersity important for eye lens function. Protein Sci. 2010; 19:1031–1043. [PubMed: 20440841]
5. Slingsby C, Clark AR. Flexible nanoassembly for sequestering non- native proteins. Structure. 2013; 21:193–194. [PubMed: 23394940]
6. Bax B, Lapatto R, Nalini V, Driessen H, Lindley PF, Mahadevan D, Blundell TL, Slingsby C. X-ray analysis of beta B2-crystallin and evolution of oligomeric lens proteins. Nature. 1990; 347:776–780. [PubMed: 2234050]
7. Van Montfort RL, Bateman OA, Lubsen NH, Slingsby C. Crystal structure of truncated human betaB1-crystallin. Protein Sci. 2003; 12:2606–2612. [PubMed: 14573871]
8. Lapatto R, Nalini V, Bax B, Driessen H, Lindley PF, Blundell TL, Slingsby C. High resolution structure of an oligomeric eye lens beta-crystallin. Loops, arches, linkers and interfaces in beta B2 dimer compared to a monomeric gamma-crystallin. J Mol Biol. 1991; 222:1067–1083. [PubMed: 1762146]

9. Najmudin S, Nalini V, Driessen HP, Slingsby C, Blundell TL, Moss DS, Lindley PF. Structure of the bovine eye lens protein gammaB(gammaII)-crystallin at 1.47 A. Acta Crystallogr D Biol Crystallogr. 1993; 49:223–233. [PubMed: 15299528]
10. Nalini V, Bax B, Driessen H, Moss DS, Lindley PF, Slingsby C. Close packing of an oligomeric eye lens beta-crystallin induces loss of symmetry and ordering of sequence extensions. J Mol Biol. 1994; 236:1250–1258. [PubMed: 8120900]
11. Takata T, Smith JP, Arbogast B, David LL, Lampi KJ. Solvent accessibility of betaB2-crystallin and local structural changes due to deamidation at the dimer interface. Exp Eye Res. 2010; 91:336–346. [PubMed: 20639133]
12. Bateman OA, Sarra R, van Genesen ST, Kappe G, Lubsen NH, Slingsby C. The stability of human acidic beta-crystallin oligomers and hetero-oligomers. Exp Eye Res. 2003; 77:409–422. [PubMed: 12957141]
13. Kim YH, Kapfer DM, Boekhorst J, Lubsen NH, Bachinger HP, Shearer TR, David LL, Feix JB, Lampi KJ. Deamidation, but not truncation, decreases the urea stability of a lens structural protein, betaB1-crystallin. Biochemistry. 2002; 41:14076–14084. [PubMed: 12437365]
14. Lampi KJ, Amyx KK, Ahmann P, Steel EA. Deamidation in human lens betaB2-crystallin destabilizes the dimer. Biochemistry. 2006; 45:3146–3153. [PubMed: 16519509]
15. Sergeev YV, Wingfield PT, Hejtmancik JF. Monomer–dimer equilibrium of normal and modified beta A3-crystallins: experimental determination and molecular modeling. Biochemistry. 2000; 39:15799–15806. [PubMed: 11123905]
16. Sergeev YV, Hejtmancik JF, Wingfield PT. Energetics of domain–domain interactions and entropy driven association of beta-crystallins. Biochemistry. 2004; 43:415–424. [PubMed: 14717595]
17. Dolinska MB, Wingfield PT, Sergeev YV. betaB1-crystallin: thermodynamic profiles of molecular interactions. PLoS One. 2012; 7:e29227. [PubMed: 22238594]
18. Chan MP, Dolinska M, Sergeev YV, Wingfield PT, Hejtmancik JF. Association properties of betaB1- and betaA3-crystallins: ability to form heterotetramers. Biochemistry. 2008; 47:11062–11069. [PubMed: 18823128]
19. Hejtmancik JF, Wingfield PT, Chambers C, Russell P, Chen HC, Sergeev YV, Hope JN. Association properties of betaB2- and betaA3-crystallin: ability to form dimers. Protein Eng. 1997; 10:1347–1352. [PubMed: 9514125]
20. Slingsby C, Bateman OA. Quaternary interactions in eye lens beta-crystallins: basic and acidic subunits of beta-crystallins favor heterologous association. Biochemistry. 1990; 29:6592–6599. [PubMed: 2397202]
21. Lampi KJ, Ma Z, Hanson SR, Azuma M, Shih M, Shearer TR, Smith DL, Smith JB, David LL. Age-related changes in human lens crystallins identified by two-dimensional electrophoresis and mass spectrometry. Exp Eye Res. 1998; 67:31–43. [PubMed: 9702176]
22. Wilmarth PA, Tanner S, Dasari S, Nagalla SR, Riviere MA, Bafna V, Pevzner PA, David LL. Age-related changes in human crystallins determined from comparative analysis of post-translational modifications in young and aged lens: does deamidation contribute to crystallin insolubility? J Proteome Res. 2006; 5:2554–2566. [PubMed: 17022627]
23. Takata T, Oxford JT, Brandon TR, Lampi KJ. Deamidation alters the structure and decreases the stability of human lens betaA3-crystallin. Biochemistry. 2007; 46:8861–8871. [PubMed: 17616172]
24. Lampi KJ, Fox CB, David LL. Changes in solvent accessibility of wild-type and deamidated betaB2-crystallin following complex formation with alphaA-crystallin. Exp Eye Res. 2012; 104:48–58. [PubMed: 22982024]
25. Zhang HM, Kazazic S, Schaub TM, Tipton JD, Emmett MR, Marshall AG. Enhanced digestion efficiency, peptide ionization efficiency, and sequence resolution for protein hydrogen/deuterium exchange monitored by Fourier transform ion cyclotron resonance mass spectrometry. Anal Chem. 2008; 80:9034–9041. [PubMed: 19551977]
26. Barbar E. NMR characterization of partially folded and unfolded conformational ensembles of proteins. Biopolymers. 1999; 51:191–207. [PubMed: 10516571]
27. Morgan JL, Song Y, Barbar E. Structural dynamics and multiregion interactions in dynein-dynactin recognition. J Biol Chem. 2011; 286:39349–39359. [PubMed: 21931160]

28. Nili M, David L, Elferich J, Shinde U, Rotwein P. Proteomic analysis and molecular modelling characterize the iron-regulatory protein haemojuvelin/repulsive guidance molecule c. Biochem J. 2013; 452:87–95. [PubMed: 23464809]

29. Gotze M, Pettelkau J, Schaks S, Bosse K, Ihling CH, Krauth F, Fritzsche R, Kuhn U, Sinz A. StavroX—a software for analyzing crosslinked products in protein interaction studies. J Am Soc Mass Spectrom. 2012; 23:76–87. [PubMed: 22038510]

30. Lampi KJ, Kim YH, Bachinger HP, Boswell BA, Lindner RA, Carver JA, Shearer TR, David LL, Kapfer DM. Decreased heat stability and increased chaperone requirement of modified human betaB1-crystallins. Mol Vis. 2002; 8:359–366. [PubMed: 12355063]

31. Takata T, Woodbury LG, Lampi KJ. Deamidation alters interactions of beta-crystallins in hetero-oligomers. Mol Vis. 2009; 15:241–249. [PubMed: 19190732]

32. Werten PJ, Carver JA, Jaenicke R, de Jong WW. The elusive role of the N-terminal extension of beta A3- and beta A1-crystallin. Protein Eng. 1996; 9:1021–1028. [PubMed: 8961355]

33. Dasari S, Wilmarth PA, Reddy AP, Robertson LJ, Nagalla SR, David LL. Quantification of isotopically overlapping deamidated and 18o-labeled peptides using isotopic envelope mixture modeling. J Proteome Res. 2009; 8:1263–1270. [PubMed: 19173613]

34. Dasari S, Wilmarth PA, Rustvold DL, Riviere MA, Nagalla SR, David LL. Reliable detection of deamidated peptides from lens crystallin proteins using changes in reversed-phase elution times and parent ion masses. J Proteome Res. 2007; 6:3819–3826. [PubMed: 17696381]

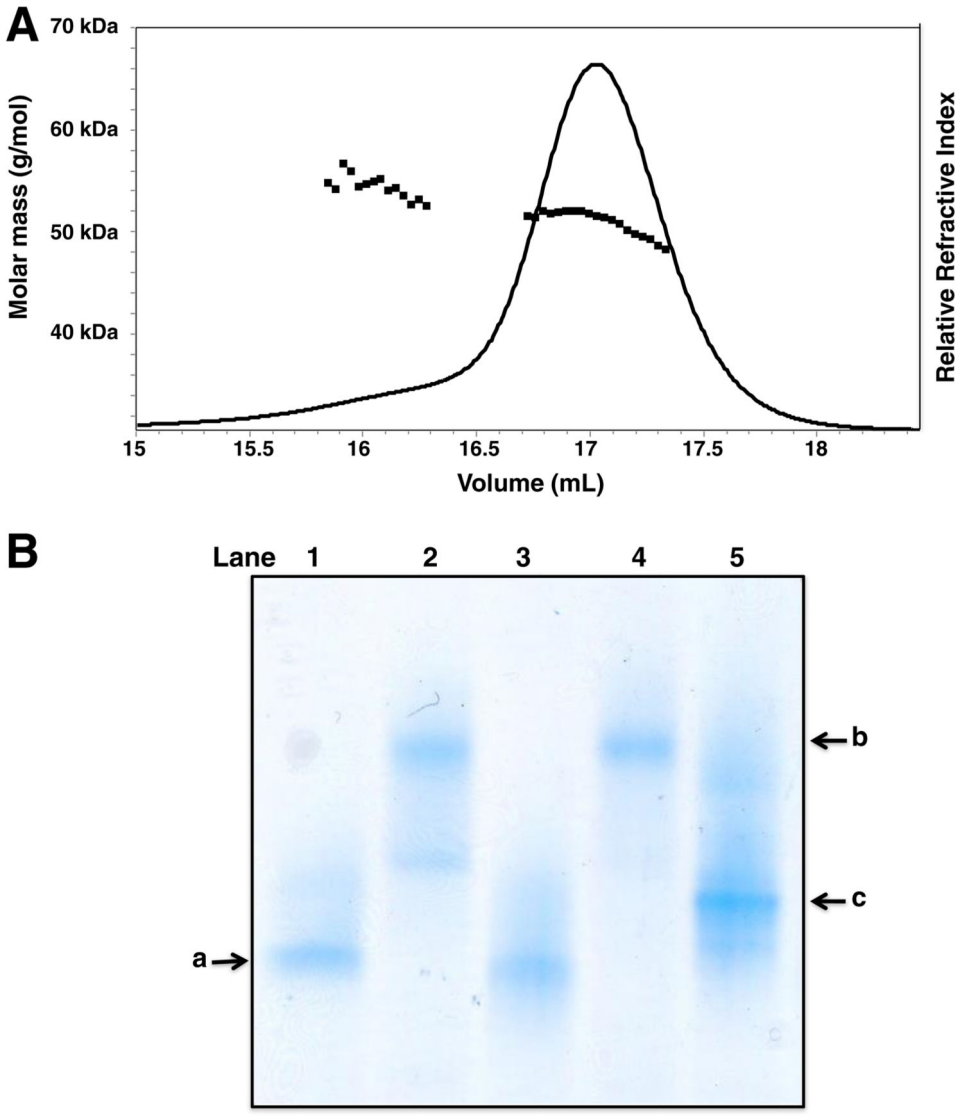

Fig. 1.

βA3 and βB2 preferentially form a heterodimer. (A) Light scattering of the βA3/βB2 heterodimer during size-exclusion chromatography in line with multiangle laser scattering. Molar masses were determined from the light scattering under the protein peak detected by the change in refractive index. (B) Blue-native polyacrylamide electrophoresis of βA3 (lane 1) and βB2 (lane 2). The same samples were incubated overnight at 37 °C, βA3 (lane 3), βB2 (lane 4), plus mixed to form βB2/βA3 (lane 5). Each lane contains 5 μg.

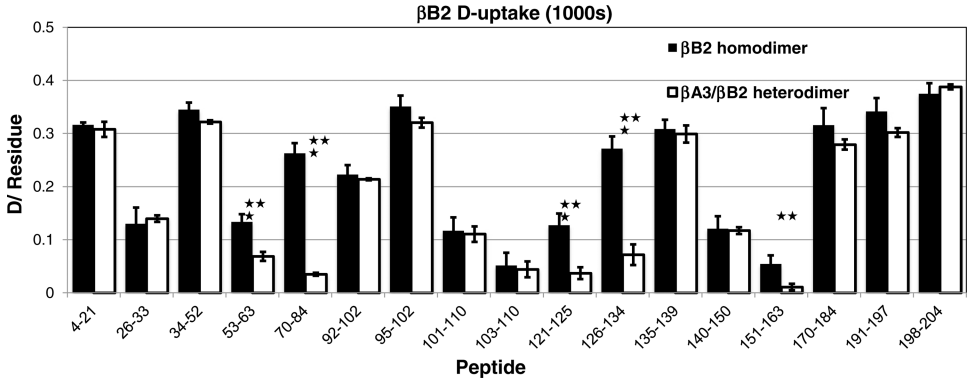

Fig. 2.

Deuterium incorporation in βB2 peptides from the βB2 homodimer and the βA3/βB2 heterodimer. Relative deuterium uptake per exchangeable residue after 1000 s of hydrogen deuterium exchange measured by mass spectrometry showing regions of solvent accessibility of βB2 alone (black bars) and in complex with βA3 (white bars). Data for representative peptides are shown from the N-terminal through the C-terminal extensions. Error bars are the standard error from an N of 3, Student's t-test, $p < 0.01$ (★★), $p < 0.001$ (★★★).

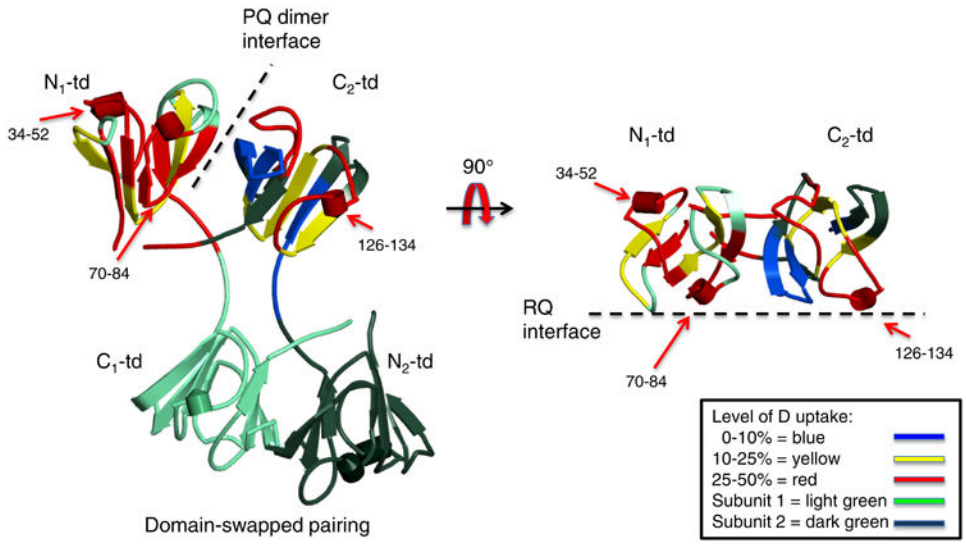

Fig. 3.

Deuterium uptake in βB2 peptides highlighted in the βB2 homodimer structure. Deuterium uptake levels from Fig. 2 are highlighted on the top half of the βB2 homodimer structure (PDB:1YTQ). The dashed line in the dimer to the left shows the interface between the two monomers, the PQ interface in the crystal structure. The dashed line to the right shows the exposed surface when the dimer is rotated down 90°, the RQ interface in the crystal structure. The C_1-td and the N_2-td are hidden from view in the structure on the right. Arrows point to peptides 70–84 and 126–134.

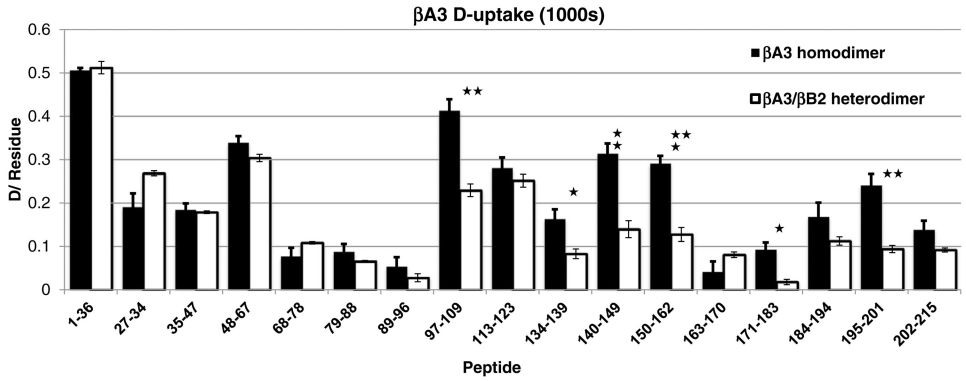

Fig. 4.

Deuterium incorporation in peptides in βA3 homodimer and in βA3 in the βA3/βB2 heterodimer. Relative deuterium uptake per exchangeable residue after 1000 s of hydrogen deuterium exchange measured by mass spectrometry showing solvent accessibility of βA3 alone (black bars) and in complex with βB2 (white bars). Data for representative peptides are shown from the N-terminal through the C-terminal extensions. Error bars are the standard error from an N of 3, Students t-test, $p < 0.05$ (★), $p < 0.01$ (★★), $p < 0.001$ (★★★).

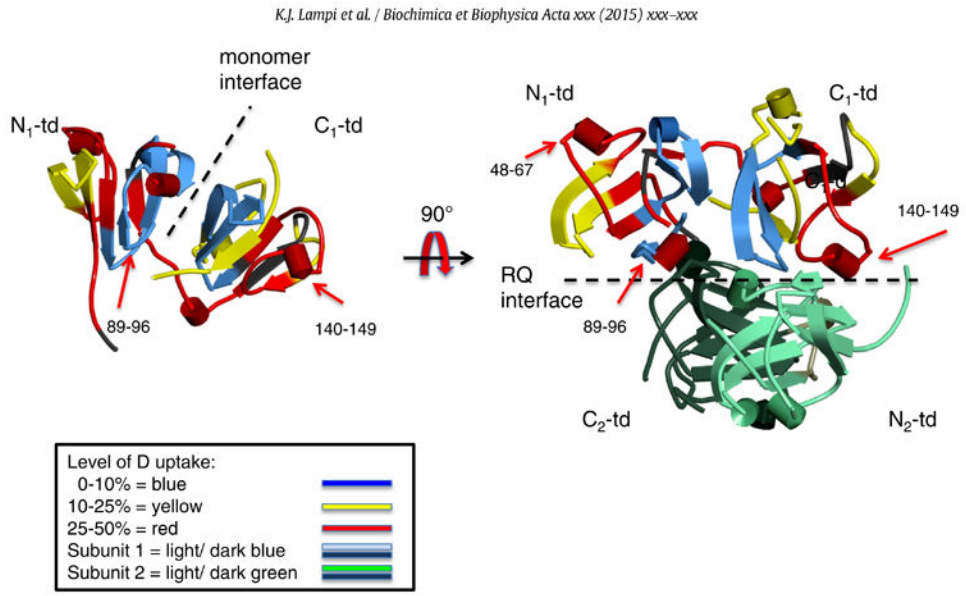

Fig. 5.

Deuterium uptake in βA3 peptides highlighted in the βA4 homodimer structure. Deuterium uptake levels from Fig. 4 are highlighted on subunit 1 of the βA4 homodimer structure (PDB: 3LWK). The dashed line in subunit 1 to the left shows the interface between the two domains (subunit 2 is hidden from view). The dashed line to the right shows the buried surface when the dimer is rotated down 90°. Arrows point to peptides 89–96 and 140–149.

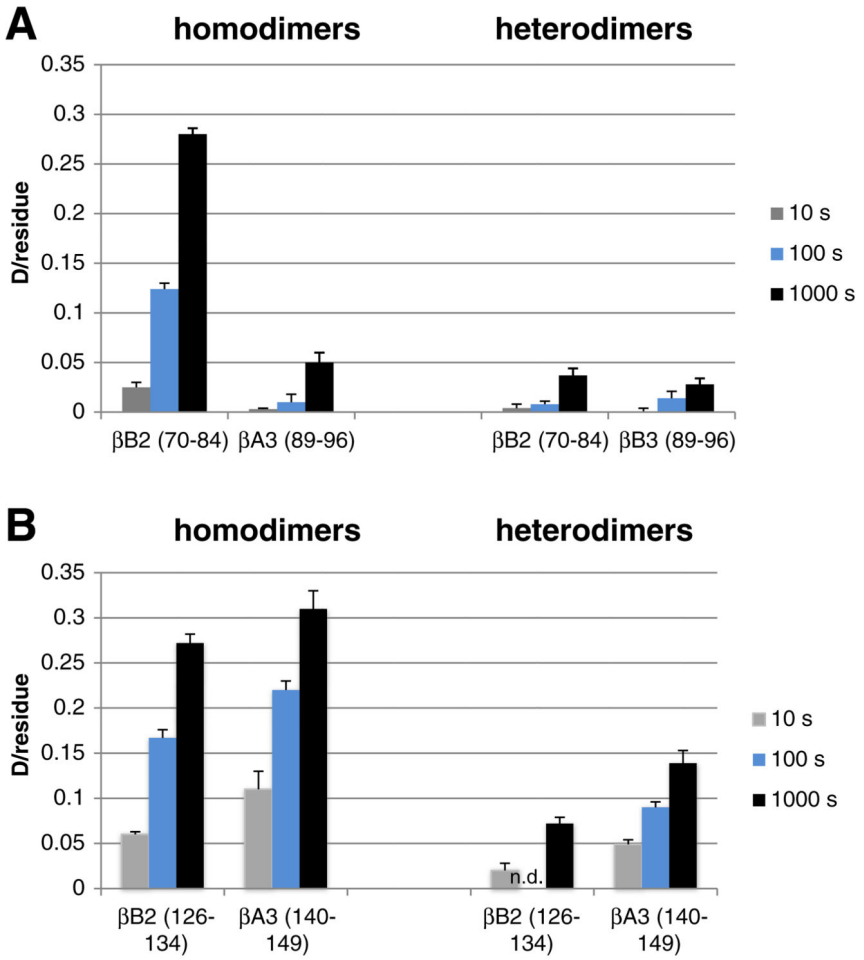

Fig. 6.

Differences in deuterium uptake in βA3 and βB2 homodimers compared to the βA3/βB2 heterodimer. Relative deuterium levels with increasing time were compared between peptides 70–84 (A) and 126–134 (B) in βB2 to the closely related peptides of 89–96 (A) and 140–149 (B) in βA3. Deuterium levels are compared for peptides in both the homodimers (left) and the heterodimers (right). nd, not detected.

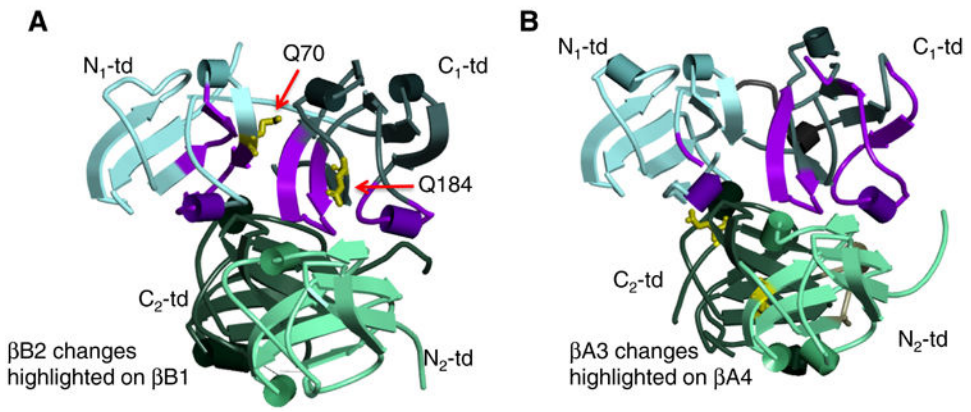

Fig. 7.

βB2 and βA3 peptides with decreased deuterium uptake in the βA3/βB2 heterodimer. (A) βB2 peptides with >40% decrease in the βA3/βB2 heterodimer compared to the βB2 homodimer are highlighted in purple in the homologous peptides in the βB1 structure (PDB: 1OKI). (B) βA3 peptides with >40% decrease in the βA3/βB2 heterodimer compared to the βA3 homodimer are highlighted in purple the homologous peptides in the βA4 structure (PDB: 3LWK). Homologous residues to Q70 in βB2 at the PQ interface between domains and Q184 in βB2 at the RQ interface between monomers are highlighted in yellow and described in the text.

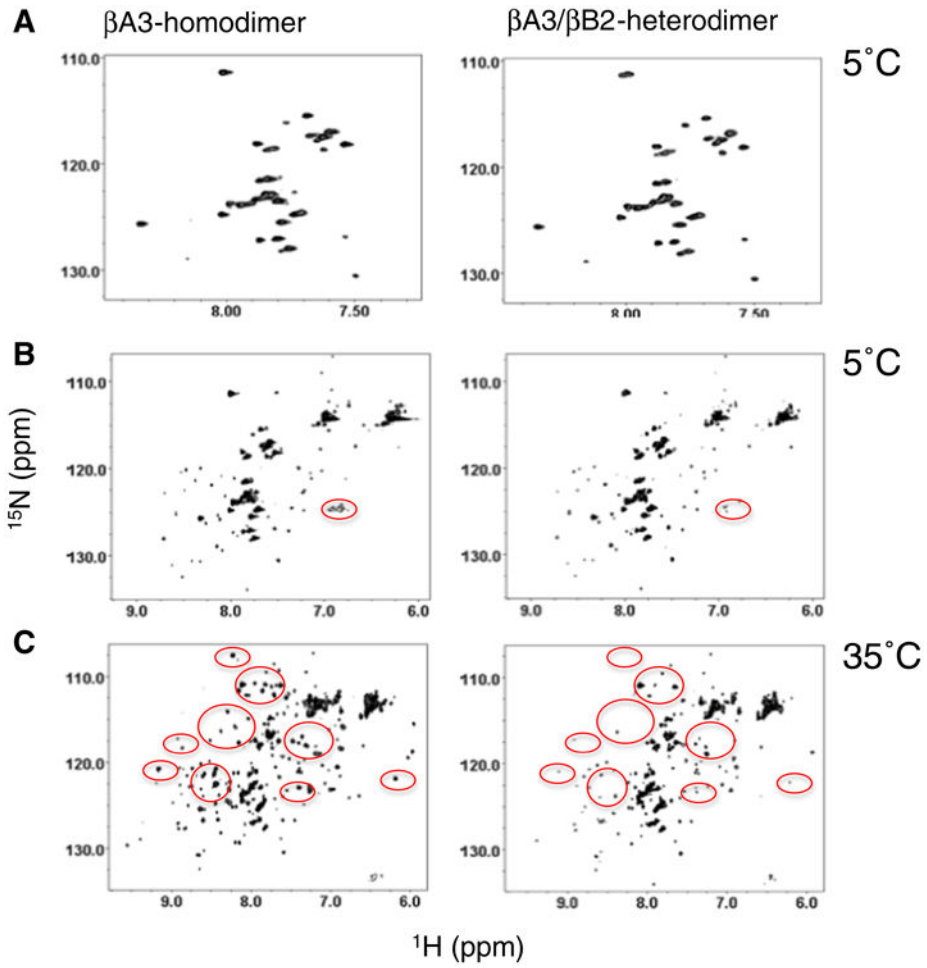

Fig. 8.

NMR spectra of ^{15}N-labeled βA3 in the βA3 homodimer (left) and the βA3–βB2 heterodimer (right). (A) NMR spectra of βA3 at 5 °C. (B) NMR spectra are shown at a lower contour level than in A to allow observation of the low intensity peaks close to the noise level. (C) NMR spectra are for the same proteins, but collected at 35 °C. Peak intensities that are significantly decreased for the heterodimer spectrum on the right compared to the homodimer on the left are circled in red.

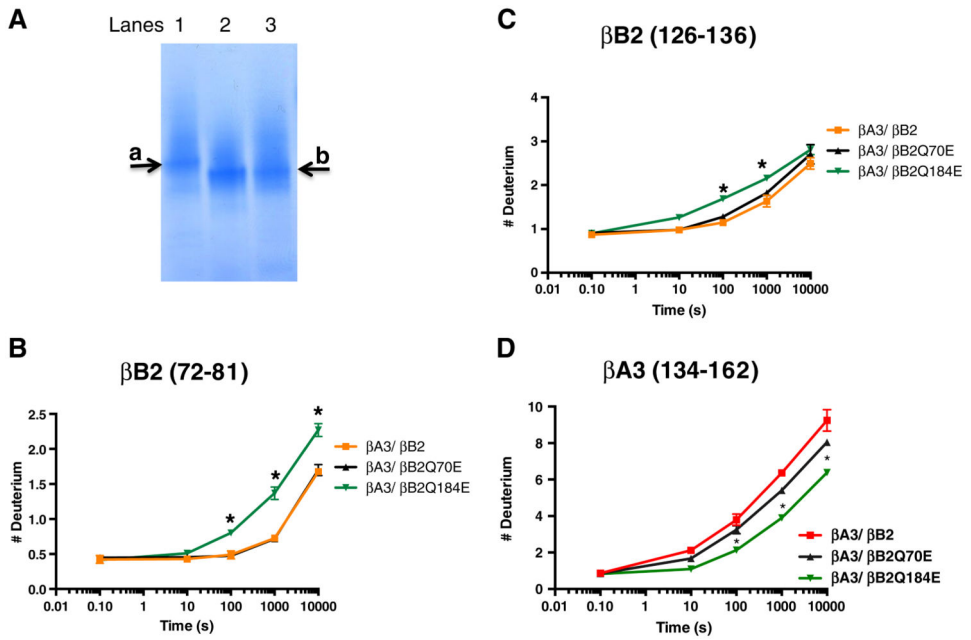

Fig. 9.

Changes in deuterium uptake in βA3/βB2 heterodimer due to deamidation in βB2. (A) Blue-native polyacrylamide electrophoresis of βA3/βB2 (lane 1), βA3/βB2Q70E (lane 2), and βA3/βB2Q184E (lane 3) after 18 h at 37 °C as in Fig. 1. Arrows denote migration of the major species in lane 1(a) and lanes 2 and 3(b). (B and C) Deuterium uptake in βB2 within βA3/βB2 (orange), βA3/βB2Q70E (black) and βA3/βB2Q184E (green). (D) Deuterium uptake in βA3 within βA3/βB2 (red), βA3/βB2Q70E (black) and βA3/βB2Q184E (green). Error bars are the standard error from an N of 3, with $p < 0.001$. (★) marking differences with βA3/βB2. Time zero was labeled sample that was immediately quenched and set at 0.1 s for visualization purposes. Time is plotted on a log scale.

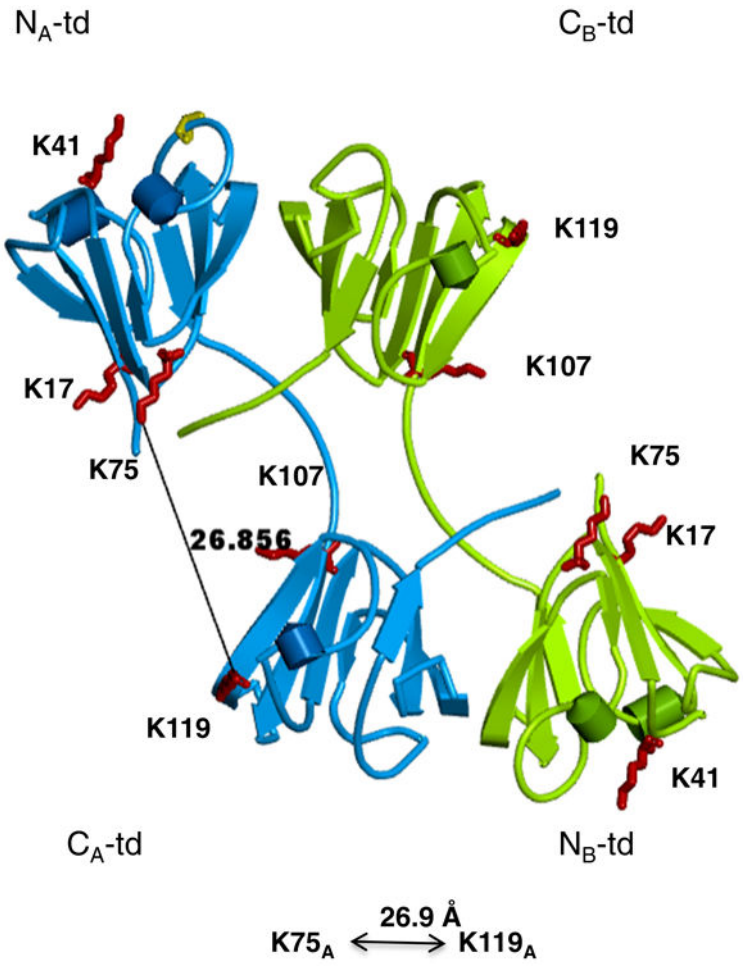

Fig. 10.

Crosslinked residues support a compact βB2 in the heterodimer with βA3. The crosslinker reagent, CBDPS, was used to crosslink nearby residues. Lys residues oriented near the surface of the RQ interface are highlighted in red. Crosslinked residues on or near this surface were identified with mass spectrometry as K75 to K119 in the heterodimer.

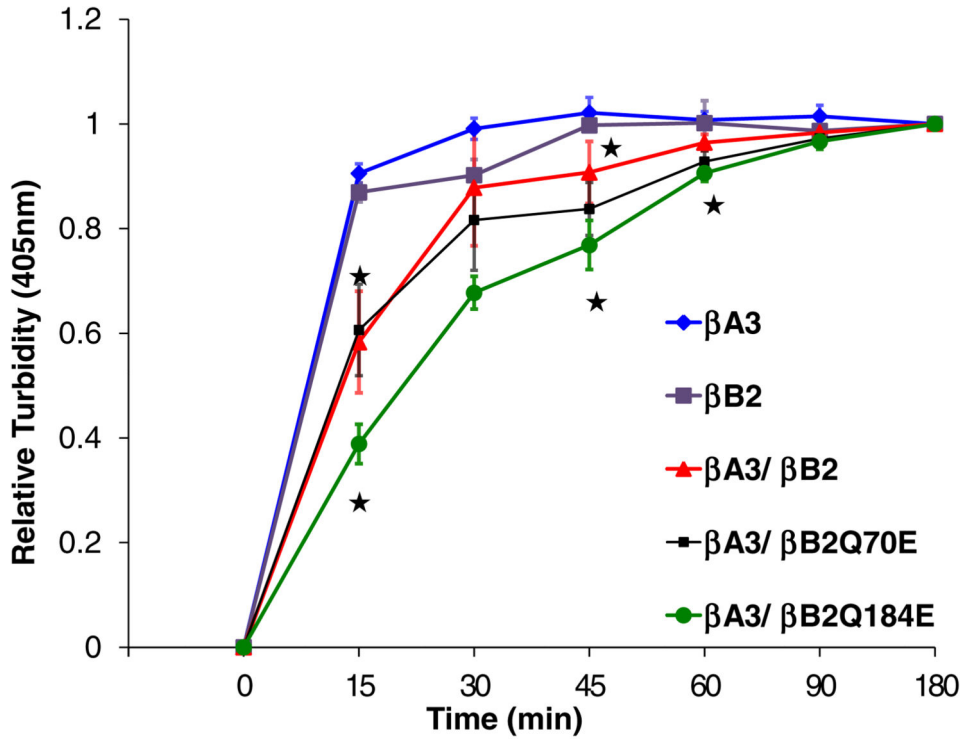

Fig. 11.

Thermal-induced denaturation of βB2, βA3, βA3/βB2, βA3/B2Q70E, and βA3/βB2Q184E. Proteins were incubated overnight at 37 °C and then subjected to 55 °C and the turbidity measured at 405 nm. Data are a percent of the OD at 180 min with N = 3 and Student's t-test with $p < 0.05$ (★) marking differences at 15 and 45 min between βA3/βB2 (red) and either homodimer (blue or purple) and at 15, 45, and 60 min between βA3/βB2Q184 (green) and βA3/βB2 (red).